Analytical and Bioanalytical Chemistry (2019) 411:591–602
https://doi.org/10.1007/s00216-018-1314-1

RESEARCH PAPER

Skip the beat: minimizing aliasing error in LA-ICP-MS measurements

Bodo Hattendorf[1] · Urs Hartfelder[2] · Detlef Günther[1]

Received: 25 May 2018 / Revised: 28 July 2018 / Accepted: 7 August 2018 / Published online: 22 August 2018

Abstract

Pulsed laser ablation sampling and sequential isotope detection can lead to signal beat in the registered signal intensities. In particular, if aerosol transport systems deliver ablated aerosol with temporal duration close to that of a single mass scan, such signal beat can become significant and lead to biased intensity ratios and concentrations. Averaging signal intensities based on the least common multiple of scan duration and laser pulse period can eliminate such a systematic bias and improve the accuracy of quantitative laser ablation experiments. The method was investigated for experiments using an ablation cell that provided aerosol washout times near 200 ms and quadrupole-based ICP-MS acquisition using different dwell and settling times that were compared with and extended by numerical simulations. It was found that the systematic bias of acquired data could exceed the inherent noise of laser ablation inductively couple plasma mass spectrometry experiments and that the averaging method could successfully minimize the bias due to beating. However, simulations revealed that this was only the case for combinations of pulse frequency and scan duration in which the number of laser pulses within the averaged period was an integer multiple of the number of isotopes in the acquisition method. In element imaging applications, this averaging will necessarily increase the size of individual pixels and it depends not only on the laser beam size but also pulse repetition rate and the acquisition settings for a sequential mass spectrometer.

Keywords Accuracy · Aliasing · Imaging · LA-ICP-MS · Sequential detection · Spectral skew

Introduction

Element imaging using laser ablation inductively coupled plasma mass spectrometry (LA-ICP-MS) is becoming increasingly popular in (bio-) chemical studies [1–8]. Laser ablation allows for targeted sampling of near-surface regions of sub-μm^3 dimensions [9], from which material is removed and transformed into aerosol particles whose composition can be determined using ICP-MS [10]. Even though the notorious "elemental fractionation" [11] can affect the quantification between different sample types, LA-ICP-MS frequently provides comparable sensitivity ratios in samples that do not differ substantially in matrix composition [12].

Advantages of LA-ICP-MS over other micro-analytical techniques like secondary ion mass spectrometry, electron probe micro-analysis or micro-X-ray fluorescence are mostly related to its specificity (i.e., relatively moderate spectral interferences), sensitivity (detection efficiencies can reach per-mil levels), and, in particular, relatively simple sample preparation requirements and flexible calibration of the element response.

The calibration of the elements' relative sensitivities in LA-ICP-MS experiments can often be carried out using reference materials of similar type. Still, the mass ablation rate of different materials even of samples with similar type can vary significantly [13] and the actual mass flow depends on the sampling conditions like laser beam diameter or laser pulse frequency. Several studies have shown that the relative elemental sensitivities vary only moderately even when the mass introduced to the ion source varies by an order or magnitude or more [12, 14]. This feature

Published in the topical collection *Elemental and Molecular Imaging by LA-ICP-MS* with guest editor Beatriz Fernández García.

Electronic supplementary material The online version of this article (https://doi.org/10.1007/s00216-018-1314-1) contains supplementary material, which is available to authorized users.

✉ Bodo Hattendorf
bodo@inorg.chem.ethz.ch

[1] Laboratory of Inorganic Chemistry, ETH Zurich, Vladimir-Prelog-Weg 1, 8093 Zurich, Switzerland

[2] Büchi Labortechnik AG, Meierseggstrasse 40, 9230 Flawil, Switzerland

makes ICP-MS attractive for laser ablation-based sampling, because the resulting changes in absolute ion signal intensities do not translate into variation of intensity or concentration ratios. By either using an internal standard of known composition in the sample or through matrix normalization procedures, accurate and precise sample compositions can often be obtained [15].

In order to meet the conditions above, however, it must be ensured that the aerosol composition and mass flow is identical for the acquisition of each isotope of interest. (Quasi-) simultaneous ion detection using time-of-flight [16–18], distance-of-flight [19, 20], or sector-field MS with detector arrays (i.e., Nier-Johnson [21] or Mattauch-Herzog geometry [22, 23]) can fulfill this condition to the highest possible degree. Most frequently, however, sequential detection using quadrupole MS or single collector sector-field instruments is employed, where the pulsed aerosol introduction can cause a so-called spectral skew [24, 25] leading to signal beat if the aerosol mass introduced varies over the duration of the mass scan. This aliasing effect is schematically shown in Fig. 1. Depending on the MS scan period and the laser pulse frequency, intensity ratios of different elements can show significant changes with time even if a homogeneous material is ablated. In order to circumvent this issue, laser ablation is often carried out using aerosol transport systems (i.e., ablation cell and transfer tubing) that induce substantial, temporal dispersion of the initial aerosol plume. By using a laser pulse frequency that ensures mixing of the individual aerosol plumes, a quasi-stationary mass flow to the ICP can be achieved and aliasing thus minimized.

With this approach, ion signal intensities registered for each isotope originate from aerosol generated by multiple laser pulses and represent a correspondingly large sample volume or mass. Consequently, intensity ratios obtained during a mass scan can only be considered to represent an integral of the variable contributions of several laser pulses. Thus, signal intensities, intensity ratios, and, ultimately, element concentrations can only be assigned to the integrated mass flow introduced into the ICP during the period of at least one mass scan. If oscillations in aerosol mass flow within this period are comparable or smaller than uncertainties of the LA-ICP-MS analysis itself (i.e., combined uncertainties of signal acquisition, ICP-MS flicker noise etc.), the impact of aliasing will likely be insignificant. This is in particular true when "bulk-like" laser ablation analyses are being performed, where a substantial number of mass scans are averaged to provide the mean concentration of the ablated material.

In imaging experiments, on the other hand, the goal is usually to assign an element's accurate concentration value to a specific sample position at the highest possible spatial resolution. Both fundamentally depend on the sampling strategy, when using ICP-MS with sequential isotope detection:

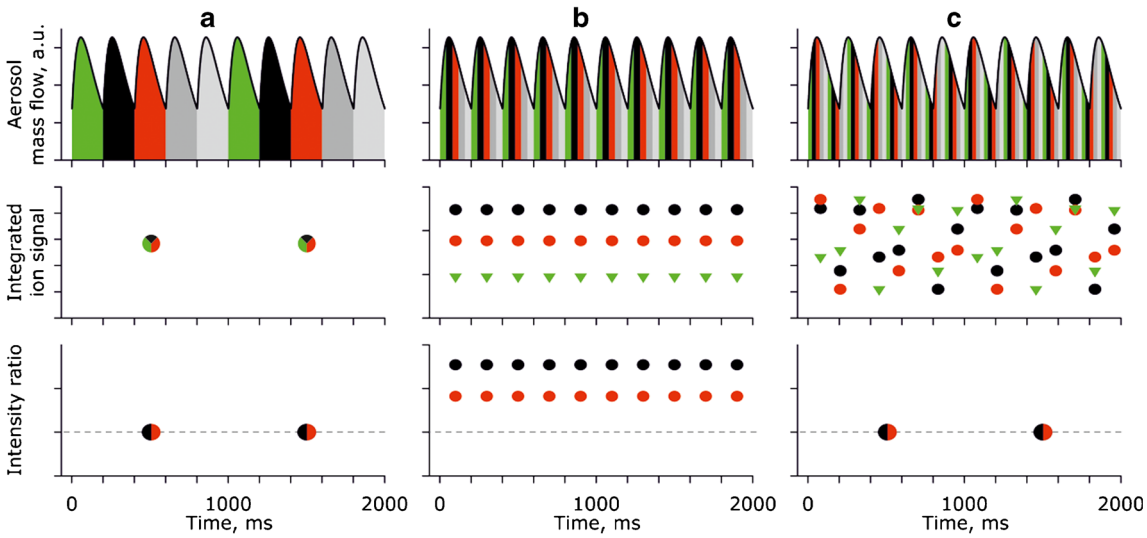

Fig. 1 Illustration of the effect of aerosol mass flow oscillation with sequential isotope detection in LA-ICP-MS experiments. The top panel shows the evolution of aerosol mass flow with time for 5 Hz laser pulse frequency. The colored regions represent isotope times of five isotopes acquired sequentially (colors represent the respective isotope times). The panels under A) correspond to a "synchronized" measurement with isotope time identical to the laser pulse period. For the center panels under B), the isotope time is 40 ms, so that the mass spectrometer scan duration is identical to the laser pulse period (in resonance). In the right panels, an isotope time of 25 ms is used. The middle row shows integrated ion signal intensities obtained for the isotopes during the mass scan (for clarity only the first three isotopes are shown), while the bottom row shows intensity ratios relative to the first isotope in the sequence for LCM averaged data. LCM periods are 1000 ms in A) (one mass scan) and C) (eight mass scans) and 200 ms in B) (one mass scan)

Single-pulse evaluation

Evaluation of one single laser pulse provides the highest confidence of the ion signals with respect to lateral position on the sample as well as depth. However, relatively low mass removal and transient aerosol mass flow rate can affect the quantification substantially. In order to ensure correlated signal intensities that allow for quantitative evaluation of the composition of the material, the changes in aerosol mass flow inside the ICP during the acquisition of a mass scan need to be sufficiently small. This can practically only be achieved by high-dispersion aerosol transport systems, which provide a transient signal duration that is longer than the mass scan (i.e., the sum of dwell and settling times of all isotopes measured). The necessary duration of the aerosol pulse depends on its shape and the number of isotopes to detect, which makes it difficult to predict. At the same time the aerosol mass flow rate is comparably small and ion signal intensities can be low. On the other hand, low-dispersion aerosol transport systems achieve higher peak intensities ratios, but signal correlation and thus quantification capabilities deteriorate. Single-pulse evaluation with high aerosol dispersion has frequently been applied in depth profiling analyses with comparably large laser beam diameters [26, 27].

Hole-drilling raster mode

In this case, a series of laser pulses is fired on a fixed sample position with a higher laser pulse frequency causing considerable mixing of the individual aerosol plumes. Because depth ablation rate per laser pulse is usually smaller than laser spot size, a "pseudo 2-D" element distribution can in principle be obtained by limiting the number of laser pulses, so that the crater depth remains smaller than its lateral dimension. Depending on laser frequency, number of pulses, and aerosol dispersion, this mode can yield quasi-stationary aerosol mass flow, which lasts at least as long as an MS scan. Due to the mixing of multiple laser pulses per mass scan, the measured intensity ratios correspond to the average of the total ablated mass during the measurement. Similar to single-pulse evaluation, data obtained using the raster mode are very specific of the lateral position but represent an average of depth.

Scanning mode ablation

When continuously moving the sample with respect to the laser beam, each laser pulse will remove material from a new lateral position and, in case of overlapping pulses (i.e., scan rate < beam diameter × laser pulse frequency), also depth. When using the same laser ablation parameters, the scanning mode will have similar characteristics of aerosol transport with respect to mass flow rate and its oscillation as the hole-drilling raster mode. High laser pulse frequencies can also lead to a quasi-stationary aerosol mass flow, which however originates from a range of depths as well as lateral positions.

A specific case of scanning mode ablation is frequently used in element imaging of biological tissue [28], when tissue thin sections are placed on a substrate and the entire depth of the tissue is removed with a single laser pulse. The aerosol mass flow in this mode has the same characteristic but ion signals are only generated from different lateral positions not depth.

While raster and scanning mode ablation can produce a quasi-stationary aerosol mass flow, pulse-related oscillations will still be present and their amplitude depends on the laser pulse frequency and the degree of aerosol dispersion in the ablation cell and transport system. Such oscillations can give rise to aliasing, which affects the quantitative description of the element distribution in imaging applications. When the transient profile of the aerosol mass flow for a single laser pulse is sufficiently reproducible [29], it may be possible to mathematically re-construct the variation of aerosol mass present in the ICP at each time of the mass scan and thereby avoid aliasing also in heterogeneous samples [30]. It remains however difficult to separate for example the contribution of an analyte in heterogeneous materials. For example, the ion signal of an analyte, occurring at high concentration in an earlier pulse but actually measured in the trailing part during the MS scan, cannot be distinguished from the contribution the same element occurring at low concentration but measured across the peak of a subsequent, overlapping pulse. Another approach to eliminate aliasing effects is to select each "isotope time" (here used to represent the sum of integration or dwell times and the settling time of the MS for the isotopes measured) to an integer multiple of the laser pulse period in order to average one or more laser pulses during the acquisition of each isotope of interest [31]. However, in this approach, changes in the concentration of elements that are not recorded within the corresponding ablated volume remain unnoticed. Another, conceptually similar, approach would be to use shorter isotope times and to average adjacent mass scans for the least common multiple (LCM) duration of mass scan and laser pulse period (further on referred to as "LCM averaging" or just "LCM"). In this case, the averaged ion signals would represent an integral of all sections of the pulse profile, albeit from different pulses. Thereby, it can be ensured that the averaged ion signal intensity of each isotope is identical to the signal intensity for the entire laser pulse as long as the mass ablation rate for the corresponding pulses is identical and the material is homogeneous in composition across the entire volume ablated. It must be ensured, however, that the timing of the acquisition is not in resonance with the laser pulse frequency.

Figure 1 illustrates this situation: In the top panel, the transient aerosol mass flow to the ICP with clearly distinguishable peaks from individual laser pulses is shown. It resembles a measurement using 5 Hz pulse repetition rate and moderate to low aerosol dispersion (< 400 ms FW0.1 M). Colored inserts

indicate the acquisition sequence for three different methods each recording signals for five isotopes. The methods only differ in the isotope times. In the leftmost sequence A), the isotope time is 200 ms (i.e., each isotope is recorded for an entire laser pulse period, or "synchronized" [31, 32]) and signal intensities for each isotope result from identical integrated aerosol mass flow. In panel B), 40 ms isotope time is used, leading to a mass spectrometer scan duration identical to the laser pulse period ("resonance"). Panel C) shows the situation for 25 ms isotope time. The middle row shows the integrated intensities for each mass scan for the first three isotopes. The bottom row displays intensity ratios of the second and third isotope measured relative to the first. The intensity ratios are calculated using LCM averaging of the raw intensities (one mass scan in A) and B) vs. eight mass scans in C)). While the methods used in A) and C) provide the correct intensity ratios after LCM averaging, it is visible that method B) results in systematic bias because all isotopes are constantly recorded from different fractions of aerosol mass introduced. Because mass spectrometer scan and laser pulse frequencies are identical, the intensity ratios are highly reproducible but heavily biased. Such a situation is most undesirable in quantitative analyses because the bias in the individual intensity ratios depends on the delay between laser pulse and the start of a mass scan, which will vary unpredictably from experiment to experiment unless a highly precise acquisition trigger can be realized. The bias occurs because the LCM of laser pulse period and mass scan duration are both 200 ms, so that the LCM only covers the aerosol from one laser pulse instead of five as required for successful LCM averaging. Method C) on the other hand produces highly variable raw intensities for the individual mass scan but, similar to Method A), LCM averaging is performed across five laser pulses and the intensity ratios obtained are identical and the ratios assume the correct value for each data point. Changes in element concentrations can in cases A) and C) only be quantified from the mean of the five laser pulses averaged. In C) however, because the mass scan duration is shorter than the laser pulse period, a change in concentration can be recognized—albeit not quantified unless signal deconvolution is employed—for each individual laser pulse. It may be noted at this stage that LCM averaging only works for averaging ion signal intensities before calculating their ratios. Average intensity ratios for the same number of sweeps would remain biased. LCM averaging of the intensity ratios of each mass scan would for example result in a mean ratio of 1.024 for the intensity ratios of isotope 2 (black) and 1.073 for the intensity ratios of isotope 3 (red) relative to isotope 1 (green).

This work aimed at evaluating the impact of the aliasing effect on quantification and its influence on the attainable spatial resolution in multi-element applications using LA-ICP-MS with sequential isotope detection. It combined experimental results obtained by LA-ICP-MS measurements of a homogeneous glass reference material (NIST SRM 610) for different combinations of laser pulse frequency, MS scan duration, and aerosol dispersion. In addition, numerical simulations of the transient signal evolution were carried out, which allowed for testing the effect for a wider range of combinations.

Experimental

Simulations

Simulation of the transient signal evolution was carried out via Microsoft Excel® spreadsheets. One sheet was used to calculate the temporal evolution of the signals for individual laser pulses ($I(t)$) based on Eq. 1) (simplified after Bleiner and Bogaerts [33]) in one column for periods of 1 ms by integration across the interval ($t - 1$ ms) t.

$$I(t) = \int_{t-1}^{t} I_0 \times k \times \left(1 - e^{-k\times(t-t_0)}\right) \times e^{-k\times(t-t_0)} \times dt \qquad (1)$$

Equation 1) represents a linear combination of two exponential terms corresponding to the rise and decay of the signal as determined by a common dispersion factor "k." The dispersion factor determines the "sharpness" of the peak and thus determines the temporal characteristics (i.e., "washout") of the aerosol transport to the ICP. t_0 in Eq. 1) represents to the start of the laser pulse and increases for subsequent pulses by the reciprocal of the laser pulse frequency. It should be noted that aliasing is merely a result of the frequency of aerosol generation and the actual function used for the modeling mostly affects the shape of the transient signals and not the occurrence of aliasing.

Simulations were carried out for three different values of k (0.001, 0.01, and 0.1), which yielded signal durations (as the width of the signal at 10% peak maximum——FW0.1M) of 3700, 370, and 37 ms, as shown in Fig. 2. These values were chosen to cover high, intermediate, and low aerosol dispersion systems, with a similar range as described in the literature [6, 34, 35]. Signal intensities from individual laser pulses were calculated in columns for positive ($t - t_0$) by incrementing the value of t_0 by the period between the pulses as given by the selected laser frequency. The calculation matrix spanned 750 columns and 15,000 rows to allow for evaluating a transient signal of 15 s with a laser pulse frequency of up to 50 Hz. Summing up the intensity values in each row yielded the total intensity created by the laser pulse train for each interval of 1 ms. Ion signals for the sequential mass spectrometry measurement were then obtained from the mean intensity within the chosen integration time in the sequence of the measurement cycle (i.e., averaging the integrated data points per line from Eq. 1 across the integration time selected). The matrix essentially simulated the transient signal created by ablation of

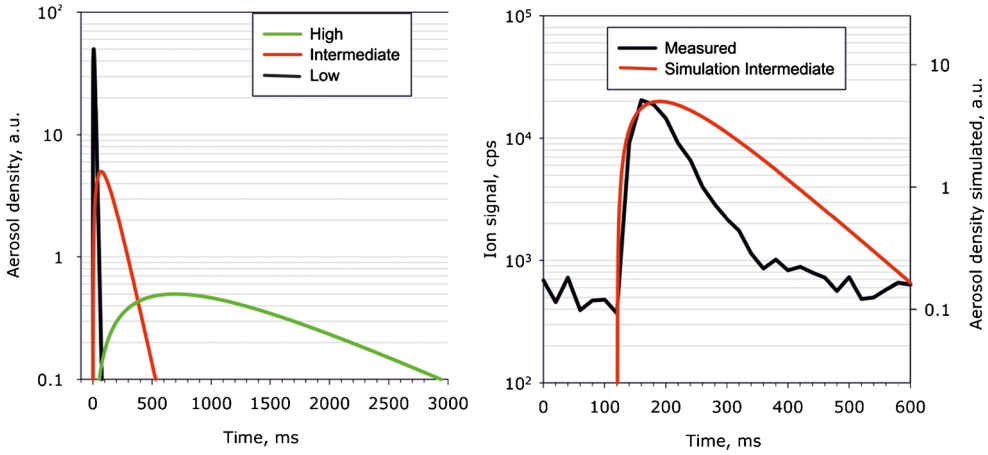

Fig. 2 Single-pulse transient signals. Simulated (left) and comparison of measurement and simulation for intermediate dispersion settings

a homogeneous material with I_0 arbitrarily set equal to 1000. All laser ablation parameters (pulse frequency and dispersion setting) as well as the integration parameters for ion signal detection (number of isotopes and integration or dwell times) could be adjusted through input fields in a "main" spreadsheet, where also the integrated isotope signals and intensity ratios were tabulated and displayed graphically. Varying the laser ablation conditions required to recalculate the entire matrix which took approximately 8 s calculation time on a conventional personal computer (Quad-core Intel® i5-4460 CPU, 3.2 GHz, 8 GB RAM, Windows 7® 64 bit, Excel® 2013). Changing acquisition parameters like dwell time or number of isotopes on the other hand required approximately 1 s for recalculation. The "main" spreadsheet contained a column listing the start time of a mass spectrometer acquisition in rows and individual columns listing the integrated signals within this "sweep" for up to 15 isotopes (more isotopes were considered in calculations when required but not displayed). Further columns were used to calculate intensity ratios of selected isotopes either on a per-sweep basis or after integrating raw intensities for a given number of sweeps according to the least common multiple (LCM) of total sweep time and laser pulse period in ms. Mean intensities of the raw transient signals, intensity ratios and LCM averaged intensities, and their ratios were evaluated together with the corresponding standard deviations to assess the impact of laser and acquisition settings on the results. A Visual Basic® script was used to automatically change input values for dispersion, laser pulse repetition rate, number of isotopes, and dwell times and to copy the resulting intensities and ratios into a separate list for further evaluation.

LA-ICP-MS measurements

Laser ablation experiments were carried out using a GeoLas Q (Microlas AG, Göttingen, Germany) 193 nm ArF-Excimer laser ablation system coupled to an Elan 6100 DRC^{plus} ICP-MS (Perkin Elmer/Sciex, Ontario, Canada). To achieve a moderate to low dispersion of the laser-generated aerosol, a predecessor of the "tube-cell" [36] configuration was employed achieving washout times of ≈ 200 ms (FW0.1 M, Fig. 2) for a carrier gas flow rate of 1 L/min He. Downstream of the ablation cell, Ar make-up gas was added via a laminar flow adapter to stabilize and optimize ICP operating conditions. Make-up gas flow rate and ion lens calibration were carried out on a daily basis, while the remaining operating conditions were kept constant throughout the experiments. Signal acquisition of the ICP-MS was performed in peak-hopping mode with 1 point/peak and identical integration times for all selected isotopes. The instrument allows for operating with quadrupole settling times of 0.2 and 3 ms respectively. Dwell times were chosen so that the isotope time spent on each individual m/Q (i.e., the sum of dwell and settling times) was integer milliseconds. The time stamps in the output data revealed that, apart from the very first scan, the majority of the scans had a duration of isotope time times the number of isotopes, with a few positive and negative deviations by 1 ms. The reason for those deviations is not clear yet. Table 1 lists the operating conditions of the LA-ICP-MS setup. All measurements were carried out using NIST SRM 610 as sample and in single-spot ablation mode. The measurement sequence included acquisition of 30 s of the gas blank and 50 s ablation. Intensity ratios of the gas blank corrected ion signals were calculated either per mass scan or after averaging according to the LCM of mass scan duration and laser pulse period.

Results

Aliasing in experimental data

The effect of sequential data acquisition on the resulting intensity ratios are exemplarily shown in the transient signal sequence in Fig. 3. Here, a laser pulse frequency of 5 Hz was used and the MS scan duration was 125 ms (five isotopes with 22 ms dwell time and 3 ms settling

Table 1 LA-ICP-MS operating conditions

ICP-MS: Elan 6100 DRC^{plus}		Laser Ablation: GeoLasQ	
RF-power	1380 W	Wavelength	193 nm
Coolant gas	17.5 L/min	Pulse duration	14 ns
Auxiliary gas	0.7 L/min	Energy density	10 J/cm2
Make-up gas (Ar)	0.84 L/min*	Beam profile	homogenized
Carrier gas (He)	1.0 L/min	Crater dia.	40 μm
Integration time	Variable	Repetition rate	variable
Settling time	3 ms, 0.2 ms		

*Optimized on a daily basis

time each). Under these conditions, a substantial oscillation was observed, for example in the signal intensities of $^{107}Ag^{+}$ shown in Fig. 3. The amplitude was found to decrease over the course of the measurement, which indicates that the dispersion of the ablated aerosol increased during the formation of the ablation crater. Intensity ratios resulting from the oscillating aerosol flow were similarly affected and the temporal changes of the ratios and amounted to up to a factor of more than 5 in this case. When using LCM averaged intensities (eight mass scans, five laser pulses, 1 s) to calculate the intensity ratios stable values could be obtained in the transient signals, which would allow for identification of even relatively small changes in concentration or isotope ratios. The standard deviation (*SD*) decreased from 58% for the raw ratios to 5.1% with LCM averaging while the standard error (*SE*, i.e., $SD/\sqrt{n}$) decreased from 3.2% ($n = 320$) to 0.8% ($n = 40$). The same trend was observed in all experiments where LCM averaging could be performed under the condition that the number of laser pulses included equalled the number of isotopes in the acquisition method.

While LCM averaging can generally reduce the scatter in the measured signal intensities and isotope ratios, it can still produce erroneous ratios when the acquisition conditions are chosen incorrectly. Table 3 shows this effect for Ag isotope ratios obtained for different combinations of laser pulse and mass scan frequencies as given in Table 2.

Three replicate measurements were carried out for each setting. The standard errors are generally similar across the repetitions and LCM averaging can lead to a substantially smaller scatter in all cases. Comparing the standard deviation (SD) of the mean ratios for the different acquisitions on the other hand shows that LCM averaging can only reduce the scatter of the data in conditions A, B, D, and E substantially. In the other cases, the individual results show a comparable spread, regardless of LCM averaging or not. These cases have in common that the number of laser pulses that contribute to an average ratio is not a multiple integer of the number of isotopes registered.

Cases C, E, and F are situations in which the mass scan duration was exactly half the laser pulse period (i.e., in resonance). As discussed above, resonance also led to comparably smaller SE of the within-run intensity ratios of the raw data but they remained biased to an unpredictable degree.

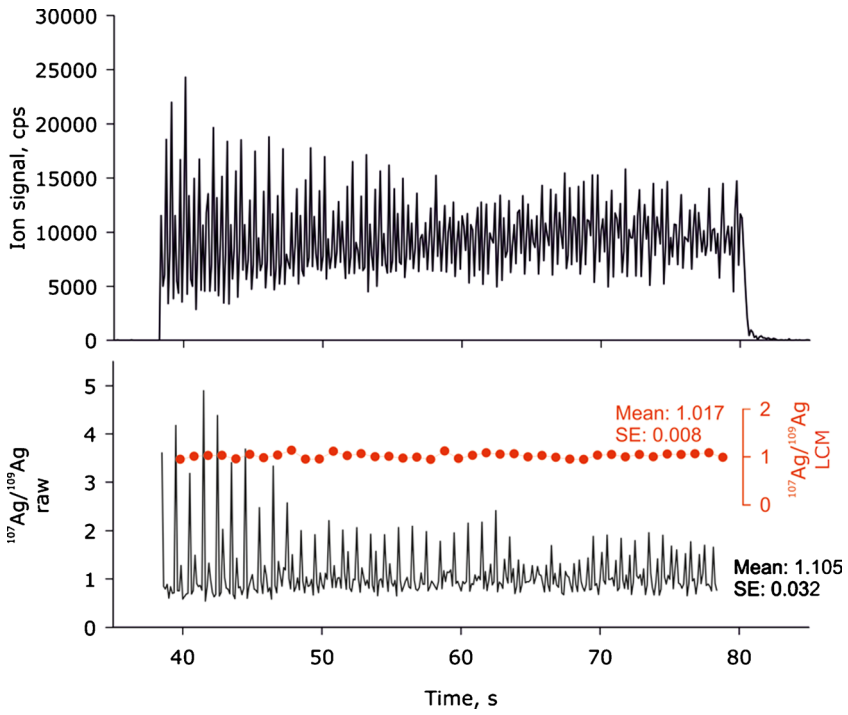

Fig`. 3 Top panel shows a typical transient signal for $^{107}Ag^{+}$ with the LA-ICP-MS setup for acquisition conditions similar to Fig. 1 right sequence: laser pulse frequency of 5 Hz, 5 isotope signals using 22 ms of dwell and 3 ms settling times. All other parameters are as given in Table 1. The lower panel shows intensity ratios for the individual MS scans (black), which exhibit the typical oscillating pattern. The data shown in red result from LCM averaged signal (1 s., eight mass scans)

Table 2 Acquisition conditions for the data shown in Table 3. Conditions A, B, D, and E fulfill the requirements for successful LCM averaging. In cases C, F, and G, the mass scan frequency (*t* MS) is exactly twice the laser pulse frequency (f_{LA}) so that 1 laser pulse is included in the average of 2 MS scans in all acquisitions. n_{ISO}: "number of isotopes in the acquisition method, t_{ISO}: "Isotope time" = dwell + settling time)

	f_{LA} Hz	n_{ISO}.	t_{ISO} ms	*f* MS Hz	LCM s	Pulses averaged*	Comments
A	5	4	8	96	0.8	4	*N* (pulses) = *N* (isotopes)
B	5	4	24	$10.41\overline{6}$	2.4	12	*N* (pulses) = 3 × *N* (isotopes)
C	5	4	25	10	0.2	1	*N* (pulses) < *N* (isotopes)
D	5	5	25	8	1.0	5	*N* (pulses) = *N* (isotopes)
E	5	9	5	$22.\overline{2}$	1.8	9	*N* (pulses) = *N* (isotopes)
F	5	10	10	10	0.2	1	*N* (pulses) < *N* (isotopes)
G	5	20	5	10	0.2	1	*N* (pulses) < *N* (isotopes)

*: Number of laser pulses included in the LCM averaged data

Numerical simulation

Simulations were carried out for a wide range of laser ablation and acquisition conditions. Laser ablation conditions comprised pulse frequencies of 2, 5, 10, 20, and 50 Hz with the three different aerosol dispersion settings and integer ms isotope times. The settings were specifically chosen to allow for mass scans and pulse periods to be integer ms values, because Excel® cannot calculate accurate LCM values from rational numbers (e.g., a laser repetition rate of 30 Hz that corresponds to a pulse period of $33.\overline{3}$ ms). The relative change of the aerosol mass flow, which represents the difference between highest and lowest signal intensities in relation to the mean, for these settings is given in Table 4.

The signal evolution was simulated for multiple isotopes (between 3 and 20) and dwell times (between 1 and 40 ms). Intensity ratios were calculated for the 2nd and 3rd isotope registered relative to isotope 1 in the mass scan sequence to evaluate the influence of the respective settings. The ratios were calculated on a per-scan basis and after LCM averaging, according to the laser pulse period and mass scan duration. Several combinations resulted in extremely long LCM periods (e.g., 2 Hz f_{LA}, 9 isotopes, and 39 ms isotope time would result in 175 s LCM) and only combinations with LCM below 3000 ms were finally considered. This is mainly because too long integration periods could exceed the time span provided by the simulation spreadsheet but also because longer averaging times are deemed unsuitable for imaging purposes. The simulation also included the "wash-in" period of the aerosol which, depending on the dispersion setting used lasted for < 10 ms (low dispersion) to almost 10 s (high dispersion). It also turned out that the scatter in the intensity ratios obtained with high-dispersion configuration reached appreciable levels only under extreme conditions (2 Hz laser pulse frequency, 40 ms isotope time) and even then remained below 2% of the mean. It is thus to be expected that other sources of error are more likely to dominate the results in these cases and the discussion here will be generally relevant only for intermediate and low-dispersion systems. In order to evaluate the stabilized signal only, the mean intensity ratios and their standard errors were calculated only for the final 7 s of the signal (i.e., resulting in at least two LCM averaged data points).

Table 5 lists the simulation results obtained for the conditions given in Table 2 for a comparison with the experimental data in Table 3. The simulation did not include variable delay between the MS scan and LA pulses to directly evaluate the occurrence of, and bias due to, resonance. The effect of resonance can however assessed via differences in the intensity ratios of individual isotopes relative to a reference in the measurement sequence. Thus data given for Repl.1–3 in Table 5 are actually the intensity ratios of three different isotopes, measured in sequence to the first isotope in the mass scan. Again intensity ratios from per-scan data and LCM averaged data are shown. While LCM averaging eliminated within-run scatter in all cases, LCM averaging could not compensate for any bias caused by a resonance setting (cases C, F and G).

A selection of simulation results for different acquisition settings using both, per-scan and LCM averaged, intensity ratios is shown in Fig. 4. The data represent isotope ratios that would be obtained with sequential LA-ICP-MS measurements under ideal conditions (no noise). Still, aliasing can cause substantial errors in quantification, in particular for low and intermediate aerosol dispersion conditions. Deviations reached up to 60% in these cases. While LCM averaging can improve quantification in many cases, resonance situations are frequent and the deviations persist. For 20 isotopes registered and 5 Hz pulse repetition rate, no situation existed in which correct intensity ratios were achieved. The deviations usually exhibited a complex trend when increasing the isotope times. More isotopes measured cause the deviations to be more pronounced and to occur at shorter isotope times for identical LA conditions. Increasing laser pulse frequency generally reduced the deviations and decreased scatter in the transient raw intensity ratios. For

Table 5 Examples of simulation results for the intermediate dispersion configuration. Laser ablation and acquisition conditions are identical to the ones used in Table 3

		Repl.1	Repl.2	Repl.3	Mean	SD	LCM1	LCM2	LCM3	Mean	SD
A	Ratio	1.004	1.016	1.032	1.0172	0.014	1	1	1	1	0
	SE	0.005	0.011	0.01			0	0	0		
B	Ratio	1.039	1.091	1.123	1.08	0.04	1	1	1	1	0
	SE	0.030	0.051	0.060			0	0	0		
C	Ratio	1.143	1.111	1.00	1.08	0.07	1.108	1.062	0.948	1.04	0.08
	SE	0.030	0.041	0.04			0	0	0		
D	Ratio	1.026	1.08	1.11	1.07	0.04	1	1	1	1	0
	SE	0.028	0.05	0.06			0	0	0		
E	Ratio	1.04	1.11	1.16	1.10	0.06	1	1	1	1	0
	SE	0.04	0.08	0.09			0	0	0		
F	Ratio	1.163	1.27	1.32	1.25	0.08	1.108	1.169	1.195	1.16	0.04
	SE	0.022	0.04	0.05			0	0	0		
G	Ratio	1.112	1.206	1.28	1.20	0.08	1.068	1.124	1.167	1.12	0.05
	SE	0.014	0.026	0.04			0	0	0		

example, for intermediate aerosol dispersion shown in the top panel in Fig. 4, the deviations would in all cases amount to less than 1% when operating at 50 Hz pulse frequency instead of 5 Hz. It also allows for more conditions that enable accurate LCM averaging. With 5 Hz LA, only 49 combinations of number of isotopes could be selected to allow for LCM averaging within 3000 ms. With 50 Hz LA this number increase to 60. Additionally, isotope times of 20 and 40 ms correspond to averaging exactly one or two pulses ("synchronous" acquisition) and provide accurate intensity ratios from a single mass scan.

When identical isotope times are used, LCM averaging can successfully avoid systematic bias provided that the following condition is fulfilled:

$$\mathrm{LCM}\ (seconds) \times f_{\mathrm{LA}} = a \times n_{\mathrm{ISO}}; a \in \mathbb{N} \quad (2)$$

Table S1 in the Electronic Supplementary Material (ESM) provides a list of combinations of laser pulse frequency as well as isotope numbers and times that fulfill the conditions for unbiased LCM averaging under these conditions. For these conditions, the number of laser pulses within the LCM is an integer multiple of the number of isotopes in the acquisition method. It ensures that all isotopes are registered at least once in the same section of the oscillating aerosol mass flow.

Consequences of aliasing in imaging applications

While the previous results indicate that LCM averaging together with a suitable combination of pulse repetition rate, the number of isotopes and isotope time can successfully eliminate the effect of aliasing in homogenous materials, the necessary averaging of ion signals originating from different laser pulses will naturally impair the detection of local concentration changes in imaging applications. Per-scan intensity ratios provide the highest temporal and thus spatial correlation in a scanning mode application, the bias due to aliasing however may cause (a) features to disappear in the noise of the measurement and (b) bias in the quantification. A numerical

Table 3 Intensity ratios obtained for $^{109}Ag^+/^{107}Ag^+$ from individual mass scans and after LCM averaging for different experimental conditions. Repl.1–3 and LCM1–3 indicate the mean intensity ratios and their standard errors obtained per-scan or after LCM averaging respectively. Mean and SD indicate the reproducibility of the intensity ratio between the three replicates

		Repl.1	Repl.2	Repl.3	Mean	SD	LCM1	LCM2	LCM3	Mean	SD
A	Ratio	1.104	1.078	1.100	1.093	0.014	1.020	1.013	1.018	1.017	0.003
	SE	0.014	0.012	0.013			0.007	0.007	0.006		
B	Ratio	1.074	1.117	1.132	1.108	0.030	0.990	0.9776	0.997	0.988	0.010
	SE	0.021	0.024	0.024			0.009	0.008	0.004		
C	Ratio	1.028	0.971	1.088	1.03	0.06	0.996	0.93	1.073	1.00	0.07
	SE	0.01	0.017	0.010			0.007	0.01	0.009		
D	Ratio	1.042	1.013	1.008	1.021	0.019	0.99	0.983	0.993	0.989	0.005
	SE	0.019	0.014	0.012			0.01	0.009	0.007		
E	Ratio	1.154	1.162	1.150	1.155	0.006	1.032	1.037	1.026	1.032	0.005
	SE	0.022	0.024	0.023			0.012	0.011	0.016		
F	Ratio	1.044	1.127	1.139	1.1	0.05	1.087	1.135	1.191	1.14	0.05
	SE	0.017	0.018	0.023			0.015	0.017	0.019		
G	Ratio	1.78	1.11	0.683	1.2	0.6	1.46	1.03	0.654	1.0	0.4
	SE	0.26	0.05	0.026			0.06	0.04	0.026		

Table 4 Relative changes of the aerosol mass flow rate for the different combinations of aerosol dispersion and laser pulse frequency used in the simulations. A value of 0.01 for example indicates that the peak to peak amplitude is 1% relative to the mean flow rate or signal intensity

	f_{LA}, Hz				
	2	5	10	20	50
High (4000 ms)	0.06	0.01	0.003	0.0007	0.0002
Intermediate (400 ms)	2.5	0.76	0.23	0.06	0.01
Low (40 ms)	25	10	5.0	2.5	0.76

simulation of such an experiment is shown as example in Fig. 5. The simulation was carried out for a constant intensity ratio of 0.8 throughout the scan except for a period of 0.4 s (corresponding to approx. The FW0.1M of the aerosol dispersion, shaded area in Fig. 5) where the ratio was 1. This corresponds for example to a 40 μm section parallel to the scan direction, traversed at 100 μm/s scan rate. With 5 Hz pulse frequency and ≤ 20 μm laser beam diameter (i.e., ≤ one pulse/position) this can cause an immediate change of the aerosol composition for just two subsequent laser pulses. Intensity ratios for such a case are shown in the left panel as black lines for per-scan intensity data, where the scatter of the ratio will barely allow for unambiguous identification of the heterogeneous section. The mean ratio observed in the unaltered section is 0.81 with a standard deviation of 0.08 and the average in the 0.4 s elevated section is 0.91 with an SD of 0.12. LCM averaging eliminated the systematic scatter in the unaltered region (mean ratio of 0.8) and would allow for a clearer identification of the elevated ratio in this case. The intensity ratio in the elevated region is 0.85 because the LCM spans over a period of 0.8 s and 2 data points were averaged to ensure that the integration covers the entire dispersed signal. Thus, the original elevated signal is essentially "diluted" four times, yielding an increase by 0.05 instead of 0.2. The shorter integration period applied for the per-scan data yields a value that is closer to the theoretical one because fewer mass scans are averaged but the mean value here is again affected substantially by aliasing. This can be seen in the right panel where the intensity ratios were simulated while moving the onset of the enriched region in steps of 25 μs across 800 μs. In practice, this corresponds to situations were a scan mode LA experiment repeatedly scans the same elevated region but with different delays between the start of the ICP-MS measurement and the onset of the laser pulses. For

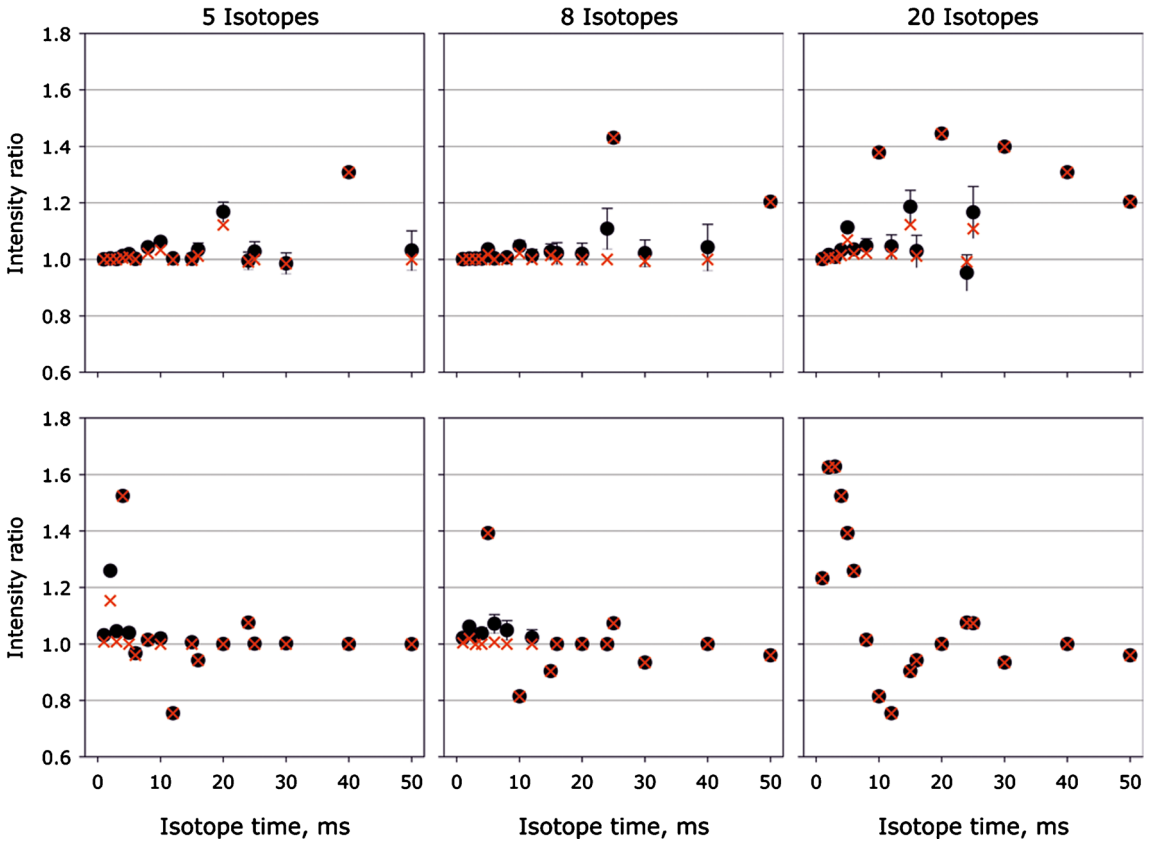

Fig. 4 Isotope ratios from numerical simulation for different LA and acquisition conditions. Black dots represent results from per-scan averaged intensity ratios and error bars indicate the corresponding SE. Red crosses are results of LCM averaged data. The top panel contains data when using intermediate dispersion of the LA generated aerosol and 5 Hz pulse repetition rate and the lower panel represents low dispersion and 50 Hz repetition rate. Ratios are plotted for 5, 8, and 20 isotopes acquired with different isotopes times

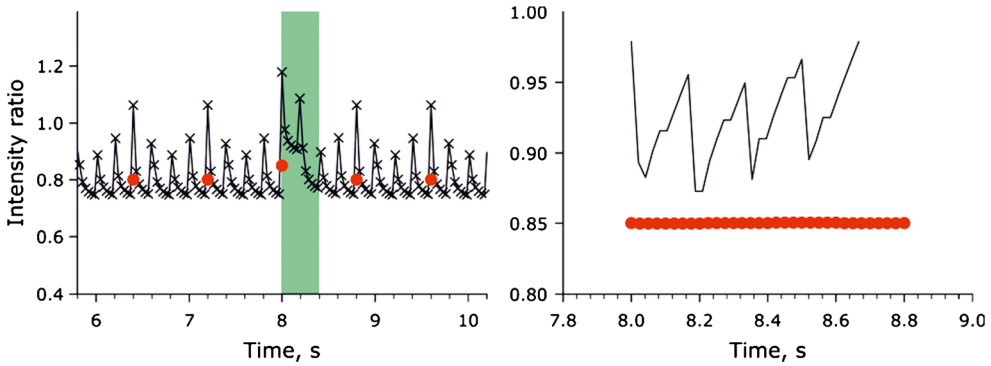

Fig. 5 Simulation of LA-ICP-MS ion signals and intensity ratios (5 Hz LA, four isotopes, 8 ms isotope time) with intermediate aerosol dispersion across a heterogeneous section. The left panel represents intensity ratios for two successively acquired isotopes. The true intensity ratio is 0.8 throughout but increases to 1 within a 500 ms period near 8 s (indicated by the shaded area). The intensity ratios are plotted for the simulations on per-scan evaluation (black line) and after LCM averaging (red dots, 800 ms LCM). The right panel shows per-scan (averaged for 400 ms) and LCM averaged intensity ratios for increasing delay of the onset of the enriched region relative to the mass spectrometer scan

LCM averaged data, the values remain practically constant throughout the experiments, while integration of only the region where the elevation is clearly visible (400 ms in this case) results again in oscillating data with an average of 0.92 and SD of 0.04, because the isotopes are registered at different points across the dispersed signal.

Variable isotope times

The previous discussion only included identical isotope times during the mass scan. Several ICP-MS instruments however may not allow for such methods. In particular, when single collector sector-field ICP-MS instruments are used, where stabilization time of the magnetic field across the mass spectrum is not constant. But also with quadrupole-based instruments, where m/Q changes can be achieved at sub-ms rates, it may be desirable to spend more time to acquire low-intensity signals to improve precision of the measurement. In all these cases, the isotope times during the mass scan may differ from another. The consequences for LCM averaging were found to become complex. The LCM for example for 5 Hz pulse repetition rate and a mass scan of five isotopes and 25 ms isotope time is the same (1 s) as for four isotopes acquired for 20 ms and one isotope with 45 ms. The LCM of the isotope with 45 ms and 5 Hz LA is however 1.8 s which is (a) longer than the LCM for the mass scan and (b) not an integer multiple of that LCM. In such cases also a systematic bias occurs in the LCM averaged intensity ratios. Changing the scan settings to four isotopes of 5 ms and one isotope of 45 ms, the LCM is 2.6 s and LCM averaging yields accurate intensity ratios again. Thus, using different isotope times in a method will most likely result in longer LCM periods to be averaged and consequently more laser pulses that need to be included in the resulting intensity ratios.

A general condition for unbiased LCM averaging with multiple dwell times could not be isolated from the numerical simulations. It appeared however that accurate intensity ratios could be obtained for a more general form of Eq. 2):

$$\mathrm{LCM}\ (seconds) \times f_{\mathrm{LA}} = a \times \sum_{i=1}^{n} \frac{(t_{\mathrm{ISO}})_i}{(t_{\mathrm{ISO}})_{min}}\ ;\frac{(t_{\mathrm{ISO}})_i}{(t_{\mathrm{ISO}})_{min}}, a \in \mathbb{N} \quad (3)$$

With $(t_{\mathrm{ISO}})_{\mathrm{i}}$ being the isotope time of isotope i and $(t_{\mathrm{ISO}})_{\mathrm{min}}$ the shortest isotope time in an acquisition method with n isotopes.

Implications for imaging applications

The results of this study confirm that aliasing can cause a substantial and systematic bias in intensity ratios if the aerosol dispersion in the LA system (as given by the FW0.1M) is approaching or below the duration of the mass scan in sequential isotope detection. It could furthermore be shown that LCM averaging can mitigate the systematic bias and thereby would yield higher accuracy for the quantitative determination of element concentration ratios. However, LCM averaged intensity ratios—similar to acquisition in "synchronous" mode—result from aerosol produced by multiple laser pulses and quantification needs to assume that the mass ablation rate for these pulses does not change substantially. Furthermore, the resulting concentration will resemble an average value of the entire mass ablated within an LCM. Thus, imaging heterogeneous sections, will cause the LCM to "distribute" the heterogeneous material over a larger period, especially when the LCM is longer than or similar to the duration of the change in concentration in the measurement. The mean concentration within the sample mass contained in the LCM is, however, unbiased. LCM averaging on the other hand cannot avoid systematic bias when LA pulses and mass scans occur in resonance. The latter situation was always found to occur when the number of laser pulses averaged over the LCM period is

not an integer multiple of the number of isotopes registered in the mass scan (for identical isotope times). For variable isotope times, the LCM was typically found to increase but the situation is more complex and a detailed analysis of the practically infinite number of combinations is beyond the scope of this manuscript.

In any case, in quantitative LA-ICP-MS imaging applications using scanning mode and sequential isotope detection, one needs to bear in mind that the size of an individual pixel in scan direction is always larger than the distance traveled during a single mass scan or the area of an individual laser pulse. The same applies to quantitative depth profiling experiments, where unbiased concentration data can only be obtained from aerosol generated by more than one laser pulse, i.e., greater depth than the mass ablation rate per pulse. Assuming that pixel size represents the spatial (or depth) resolution of the resulting images, there are several aspects that affect the attainable resolution, which are not only related to the laser ablation conditions applied. The smallest voxel size achievable also depends on the thickness of the material ablated. If the material is not entirely removed by the LA scan, each voxel represents the composition of a sample volume corresponding to dimensions of:

$$x = v_{scan} \times LCM + l_x, y = l_y \text{ and } z = r \times f_{LA} \times l_x / v_{scan.}$$

Here v_{scan} is the scan rate, l_x and l_y are the dimensions of the laser beam in scan direction (x) and in perpendicular respectively, r is the depth ablation rate, and f_{LA} the laser pulse repetition rate.

For a given LCM period, the lateral image resolution will thus improve only by decreasing the scan rate, which in turn increases the depth of the ablated track.

If the material is thinner than the resulting value of z, like in experiments where a tissue slice on a substrate are ablated by a single laser pulse, the lateral resolution can be lowered to below the laser spot dimensions if $v_{scan} \times LCM < l_x$. In such a case and when rectangular laser spots are used, the voxel size would be given by

$$x = v_{scan} \times LCM, y = \Delta_y \text{ and } z = d < r \times f_{LA} \times l_x / v_{scan.}$$

Here, Δ_y is the displacement of two adjacent scan lines and d the material's thickness.

Here, the voxel size is also a function of the scan rate and with a lower translation speed, smaller pixel sizes can be realized. It will thus ultimately be the result of finding a compromise between image size and measurement time.

Conclusion

The systematic bias caused by aliasing, which leads to signal beat in sequential isotope detection with pulsed sample introduction by laser ablation, can successfully be avoided by LCM averaging of the recorded ion signal intensities. Signal beat can become particularly pronounced for LA systems with minimized aerosol dispersion, which have become increasingly popular for imaging applications. The higher the amplitude of the aerosol mass flow oscillation into the ICP, the more pronounced bias will occur. Selecting appropriate acquisition conditions one can, however, register a transient signal which corresponds to the entire oscillation of the aerosol mass flow, while originating from subsequent laser pulses. Averaging of ion signal intensities across the LCM of mass scan duration and laser pulse period then can be used to calculate non-biased intensity ratios and ultimately concentration ratios that represent the average composition of the material ablated during one LCM. Even though this method will increase the pixel or voxel size of the image compared to intensity ratios calculated from per-scan ion signals, it is free of a systematic bias in the quantitative data associated with the latter. LCM averaging requires a match of the MS acquisition and the laser ablation pulse period. Additionally, LCM averaged data are not always free of bias. Bias is only avoided if the number of laser pulses included in the LCM period is an integer multiple of the number of isotopes registered. This limits the combination of isotopes and dwell times that can provide non-biased data. The method of LCM averaging is essentially a variant of selecting dwell plus settling times so that they equal the laser pulse period. The use of shorter dwell is however advantageous in that also features that may be causing changes in the aerosol composition within successive laser pulses can more likely be identified and quantified. LCM averaging may be further useful to improve isotope ratio measurement precision with single collector ICP-MS instrument and laser ablation sampling, when using laser ablation sampling with short or intermediate aerosol washout laser ablation cells.

Acknowledgements Roland Mäder is very much thanked for designing and manufacturing the ablation cell that made the experiments possible.

Funding information This work was made possible by funding from the ETH Zurich.

Compliance with ethical standards

Conflict of interest The authors declare that they have no conflict of interest.

References

1. Becker JS, Zoriy MV, Dehnhardt M, Pickhardt C, Zilles K. Copper, zinc, phosphorus and sulfur distribution in thin section of rat brain tissues measured by laser ablation inductively coupled plasma mass spectrometry: possibility for small-size tumor analysis. J Anal At Spectrom. 2005;20(9):912.

2. Woodhead J, Swearer S, Hergta J, Maasa R. In situ Sr-isotope analysis of carbonates by LA-MC-ICP-MS: interference corrections, high spatial resolution and an example from otolith studies. J Anal At Spectrom. 2005;20(1):22–7.
3. Seuma J, Bunch J, Cox A, McLeod C, Bell J, Murray C. Combination of immunohistochemistry and laser ablation ICP mass spectrometry for imaging of cancer biomarkers. Proteomics. 2008;8(18):3775–84.
4. Fernandez B, Costa JM, Pereiro R, Sanz-Medel A. Inorganic mass spectrometry as a tool for characterisation at the nanoscale. Anal Bioanal Chem. 2010;396(1):15–29.
5. Hare D, Austin C, Doble P, Arora M. Elemental bio-imaging of trace elements in teeth using laser ablation-inductively coupled plasma-mass spectrometry. J Dent. 2011;39(5):397–403.
6. Wang HA, Grolimund D, Van Loon LR, Barmettler KD, Borca CN, Aeschlimann B, et al. High spatial resolution quantitative imaging by cross-calibration using laser ablation inductively coupled plasma mass spectrometry and synchrotron micro-X-ray fluorescence technique. Chimia. 2012;66(4):223–8.
7. Burger M, Gundlach-Graham A, Allner S, Schwarz G, Wang HA, Gyr L, et al. High-speed, high-resolution, multielemental LA-ICP-TOFMS imaging: part II. Critical evaluation of quantitative three-dimensional imaging of major, minor, and trace elements in geological samples. Anal Chem. 2015;87(16):8259–67.
8. Waentig L, Roos PH, Jakubowski N. Labelling of antibodies and detection by laser ablation inductively coupled plasma mass spectrometry. J Anal At Spectrom. 2009;24(7):924–33.
9. Giesen C, Wang HA, Schapiro D, Zivanovic N, Jacobs A, Hattendorf B, et al. Highly multiplexed imaging of tumor tissues with subcellular resolution by mass cytometry. Nat Methods. 2014;11(4):417–22.
10. Perkins WT, Pearce NJG, Westgate JA. The development of laser ablation ICP-MS and calibration strategies: examples from the analysis of trace elements in volcanic glass shards and sulfide minerals. Geostand Newslett. 1997;21(2):175–90.
11. Fryer BJ, Jackson SE, Longerich HP. Design, operation and role of the laser ablation micrprobe coupled with an inductively coupled plasma mass spectrometer (LAM-ICP-MS) in the earth sciences. Can Mineral. 1995;33:303–12.
12. Kroslakova I, Günther D. Elemental fractionation in laser ablation-inductively coupled plasma-mass spectrometry: evidence for mass load induced matrix effects in the ICP during ablation of a silicate glass. J Anal At Spectrom. 2007;22(1):51–62.
13. Horn I, Guillong M, Gunther D. Wavelength dependant ablation rates for metals and silicate glasses using homogenized laser beam profiles - implications for LA-ICP-MS. Appl Surf Sci. 2001;182(1–2):91–102.
14. Fietzke J, Frische M. Experimental evaluation of elemental behavior during LA-ICP-MS: influences of plasma conditions and limits of plasma robustness. J Anal At Spectrom. 2016;31(1):234–44.
15. Jochum KP, Stoll B, Weis U, Jacob DE, Mertz-Kraus R, Andreae MO. Non-matrix-matched calibration for the multi-element analysis of geological and environmental samples using 200 nm femtosecond LA-ICP-MS: a comparison with nanosecond lasers. Geostand Geoanal Res. 2014;38(3):265–92.
16. Bleiner D, Hametner K, Günther D. Optimization of a laser ablation-inductively coupled plasma "time of flight" mass spectrometry system for short transient signal acquisition. Fresenius J Anal Chem. 2000;368(1):37–44.
17. Leach AM, Hieftje GM. Standardless semiquantitative analysis of metals using single-shot laser ablation inductively coupled plasma time-of-flight mass spectrometry. Anal Chem. 2001;73(13):2959–67.
18. Burger M, Schwarz G, Gundlach-Graham A, Käser D, Hattendorf B, Günther D. Capabilities of laser ablation inductively coupled plasma time-of-flight mass spectrometry. J Anal At Spectrom. 2017;32(10):1946–59.
19. Gundlach-Graham A, Dennis EA, Ray SJ, Enke CG, Barinaga CJ, Koppenaal DW, et al. Laser-ablation sampling for inductively coupled plasma distance-of-flight mass spectrometry. J Anal At Spectrom. 2015;30(1):139–47.
20. Dennis EA, Ray SJ, Enke CG, Gundlach-Graham AW, Barinaga CJ, Koppenaal DW, et al. Distance-of-flight mass spectrometry with IonCCD detection and an inductively coupled plasma source. J Am Soc Mass Spectrom. 2016;27(3):371–9.
21. Stirling CH, Lee DC, Christensen JN, Halliday AN. High-precision in situ U-238-U-234-Th-230 isotopic analysis using laser ablation multiple-collector ICPMS. Geochim Cosmochim Acta. 2000;64(21):3737–50.
22. Burgoyne TW, Hieftje GM, Hites RA. Design and performance of a plasma-source mass spectrograph. J Am Soc Mass Spectrom. 1997;8(4):307–18.
23. Barnes JH, Schilling GD, Hieftje GM, Sperline RP, Denton MB, Barinaga CJ, et al. Use of a novel array detector for the direct analysis of solid samples by laser ablation inductively coupled plasma sector-field mass spectrometry. J Am Soc Mass Spectrom. 2004;15(6):769–76.
24. Günther D, Horn I, Hattendorf B. Recent trends and developments in laser ablation-ICP-mass spectrometry. Fresenius J Anal Chem. 2000;368(1):4–14.
25. Schilling GD, Andrade FJ, Barnes JH, Sperline RP, Denton MB, Barinaga CJ, et al. Continuous simultaneous detection in mass spectrometry. Anal Chem. 2007;79(20):7662–8.
26. Bleiner D, Plotnikov A, Vogt C, Wetzig K, Günther D. Depth profile analysis of various titanium based coatings on steel and tungsten carbide using laser ablation inductively coupled plasma – "time of flight" mass spectrometry. Fresenius J Anal Chem. 2000;368(2–3):221–6.
27. Plotnikov A, Vogt C, Hoffmann V, Taschner C, Wetzig K. Application of laser ablation inductively coupled plasma quadrupole mass spectrometry (LA-ICP-QMS) for depth profile analysis. J Anal At Spectrom. 2001;16(11):1290–5.
28. Moreno-Gordaliza E, Giesen C, Lazaro A, Esteban-Fernandez D, Humanes B, Canas B, et al. Elemental bioimaging in kidney by LA-ICP-MS as a tool to study nephrotoxicity and renal protective strategies in cisplatin therapies. Anal Chem. 2011;83(20):7933–40.
29. Bleiner D, Günther D. Theoretical description and experimental observation of aerosol transport processes in laser ablation inductively coupled plasma mass spectrometry. J Anal At Spectrom. 2001;16(5):449–56.
30. Van Malderen SJM, van Elteren JT, Šelih VS, Vanhaecke F. Considerations on data acquisition in laser ablation-inductively coupled plasma-mass spectrometry with low-dispersion interfaces. Spectrochim Acta B. 2018;140:29–34.
31. Hutchinson RW, McLachlin K, O'Connor C, editors. Better imaging analysis by LA-ICP-MS – an analyst's toolkit. European Winter Conference on Plasma Spectrochemistry; 2013; Krakow.
32. van Elteren JT, Selih VS, Sala M, Van Malderen SJM, Vanhaecke F. Imaging artifacts in continuous scanning 2D LA-ICPMS imaging due to nonsynchronization issues. Anal Chem. 2018;90(4):2896–901.
33. Bleiner D, Bogaerts A. Computer simulations of laser ablation sample introduction for plasma-source elemental microanalysis. J Anal At Spectrom. 2006;21(11):1161–74.
34. Feldmann I, Koehler CU, Roos PH, Jakubowski N. Optimisation of a laser ablation cell for detection of hetero-elements in proteins blotted onto membranes by use of inductively coupled plasma mass spectrometry. J Anal At Spectrom. 2006;21(10):1006–15.
35. Van Malderen SJM, Managh AJ, Sharp BL, Vanhaecke F. Recent developments in the design of rapid response cells for laser ablation-inductively coupled plasma-mass spectrometry and their impact on bioimaging applications. J Anal At Spectrom. 2016;31(2):423–39.
36. Wang HA, Grolimund D, Giesen C, Borca CN, Shaw-Stewart JR, Bodenmiller B, et al. Fast chemical imaging at high spatial resolution by laser ablation inductively coupled plasma mass spectrometry. Anal Chem. 2013;85(21):10107–16.